Kinetic Modelling on Solid State Reduction of Chromite Pellet with CO

Yanping XIAO and Lauri HOLAPPA

Laboratory of Metallurgy, Helsinki University of Technology
P.O. Box 6200, FIN-02015 HUT, Finland

Abstract

In the present paper, a modified structural grain model is developed for simulating the chromite pellet reduction with CO. The reducibility of the chromite constitutes with CO is analysed based on the thermodynamic calculation. The principles and the mathematical expressions of the kinetic reaction model are introduced. The experimental verifications, the calculation results, and the reaction mechanisms are discussed. In this reaction model, the sintering effect is considered. The calculated reduction rate agrees fairly well with the experimental measurements. In the modelling, the concentration profile of CO and the reaction front movement of the chromite grains inside the pellet can be calculated. The effects of the pellet porosity, pellet size as well as the chromite grain size on the reduction rate are predicted with the model calculations.

Introduction

Chromite reduction with CO gas is of practical significance in FeCr production process. Chromite pellet reduction with CO is a complex non-catalytic gas-solid reaction. The mathematical modelling of the reaction system is important for interpreting the experimental data on laboratory scale, and further for providing a kinetic aid to the FeCr process modelling. The mathematical modelling work on this reaction system is not yet available. According to the literature, numerous reaction models have been proposed to simulate different gas-solid reactions, and may be roughly categorised as non-structural and structural models. The non-structural models usually do not take the structural parameters of the solid into considerations, and mainly utilise apparent rate constants and diffusivities, for example, unreacted core model (1), two stage model (2), and zone reaction model (3). The structural models consider the structural properties including porosity, density and grain size, and the reaction rate constants and diffusion coefficients could be determined independently, such as pore models (4), grain models (5) and volume reaction models (6).

In previous work of this project (7), the unreacted core model was applied for discussing the reaction mechanism of C-containing chromite pellet. This model is mainly for the dense particles and obviously can not be applied directly to describe chromite pellet reduction with CO gas. According to the experimental observations on the reduction of Outokumpu Tornio chromite pellet with CO (7), metallic droplets were found both in inner part and outer part of the chromite pellet with different Fe/Cr ratio. Some of the chromite particles within the pellet were observed to be with certain product layer. Based on the experimental information, a modified grain model was developed to mathematically simulate the chromite pellet reduction with CO in the present work. It is assumed that the pellet is made up of a certain amount of grains, and the overall reduction rate is contributed by all these individual grains. The present paper will first analyse the thermodynamic possibilities of chromite reduction with CO, then introduce the principles and the mathematical expressions of the reaction models. Followed, the coupling factors with chromite pellet reduction and the experimental verifications as well as the predicted calculation results will be presented. Meanwhile, the reaction mechanisms and the model characteristics will be discussed.

Thermodynamic analysis on the chromite reduction with CO

In general, chromite contains iron chromite ($FeCr_2O_4$), picrochromite ($MgCr_2O_4$), magnetite ($FeFe_2O_4$), magnesium aluminate ($MgAl_2O_4$) and some silicate phases. In order to consider the reduction process of the chromite with CO in detail, it is necessary to thermodynamically analyse the reaction possibilities. According to the chromite composition from Outokumpu Tornio and the thermodynamic calculations on the reduction of the main constituents of chromite with CO, the fraction of the reducible oxygen in each reducible constitute to that in the chromite, the reaction heat and the equilibrium constant were calculated and listed in Table 1. The reaction heat was calculated based on the heat capacity of the reaction components (9). The equilibrium partial pressure ratio of CO_2 to CO is represented in Fig. 1 in the temperature range of 1623 to 1923 K. The activities of the solid reactants and products were assumed to be unity in the calculation. It can be seen that chromite pellet reduction with CO is a very complicated process, it needs very high CO partial pressure, and iron oxides will react more rapidly with the gas, and the chromium oxides may undergo a slower reaction.

By comparing the equilibrium oxygen partial pressure, it was found that the reduction of $MgCr_2O_4(s)$ needs higher starting temperature than that of $FeCr_2O_4(s)$. At the same temperature, the reduction tendency of $FeCr_2O_4(s)$ is much bigger than that of $MgCr_2O_4(s)$, i.e., $FeCr_2O_4(s)$ is easier to be reduced than $MgCr_2O_4(s)$. Similarly, $FeFe_2O_4(s)$ is easier to be reduced than $FeCr_2O_4(s)$. According to the information on the reduction degrees of iron and chromium in

the chromite in literature (10), before the start of the chromium oxide reduction, about 40% of iron oxides has been reduced. Be-

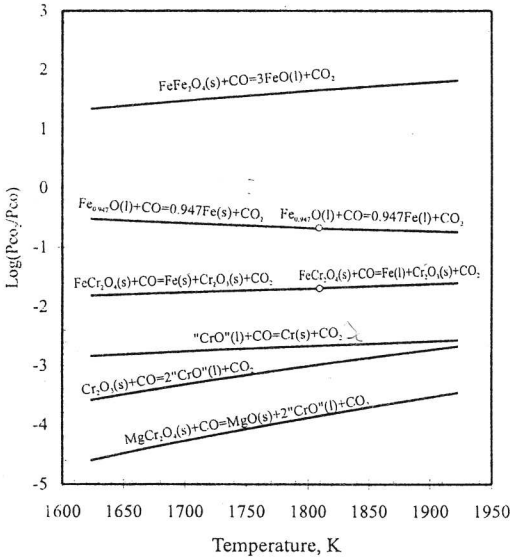

Fig.1. Equilibrium partial pressure ratio of CO_2 to CO for the reduction of the main constituents of chromite by CO.

/ond that limit, the iron oxides and chromium oxide are reduced ;imultaneously. How to consider multi-solid reactants in a reaction nodel is a challenging subject. In the present work, this chemical reaction characteristics was described by an average equilibrium constant in a macro-level which is determined based on reaction temperature, reduction degree, chromite composition, and different equilibrium constants for the possible reactions of the reducible constitutes in chromite.

Reaction model

General Considerations

The reduction reaction actually takes place between gases and porous solids which are characterised by different interrelated mechanisms or steps. Because the pellet is porous, the micro-level factors, such as ionic diffusion, new phase formation and the rearrangement of the cations and anions were ignored. In general, the reactions involving a gas and a pellet with porous solid can be analysed as follows:

1. mass transfer of gaseous reactant through an external gas film surrounding the solid pellet;
2. diffusion of the gaseous reactant through the pellet pores, and further through the porous solid which consists of a mixture of solid reactants and products;
3. adsorption of the gaseous reactant on the surface of solid reactant;
4. chemical reaction at the surface of the solid reactant;
5. desorption of the gaseous product from the surface of solid product;
6. diffusion of the gaseous product through the solid phase and through the pellet pores from the interior to the pellet surface;
7. mass transfer of gaseous product through the external gas film to ambient gas stream.

In addition, due to the existence of the chemical reaction heat, the heat transfer will accompany the reaction and diffusional steps:

1. convective and radiative heat transfer between the gas stream and the external solid surface;
2. conductive heat transfer within the pellet.

The significance of each step in the overall reaction depends on the reaction system and the specific experimental conditions.

Model Construction

In the present reaction model, it is assumed that a spherical pellet of the solid reactant consists of a large number of spherical chromite particle grains with uniform size which are surrounded by pores. The pellet sample is brought into contact with a reacting gas CO to form a solid product and a gaseous product CO_2. The rate of adsorption and desorption of the reaction gas on the solid lattice is much faster than the chemical reaction rate. The reaction of each grain is assumed to follow the unreacted core model (7), i.e., to proceed from the outer surface toward the centre inside, the reaction front forming spherical symmetry within each grain. The re-

Table 1. Thermodynamic Calculations of Different Oxide Species in Chromite

Reactions	$\Delta G°$, J (8)	ρ_i/ρ_m	T, K	ΔH_i, J	K_E^i
$FeFe_2O_4(s)+CO=3FeO(l)+CO_2(g)$	94384-80.8T	0.0206	1693	-109375	29.5
			1793	-132433	42.8
$Fe_{0.947}O(l)+CO=0.947Fe(s)+CO_2(g)$	-48530+39.8T	0.0619	1693	-14657	0.261
			1793	-14483	0.215
$FeCr_2O_4(s)+CO=Fe(s)+CO_2(g)+Cr_2O_3(s)$	35739+12.6T	0.189	1693	41145	0.0172
			1793	41217	0.0198
$Cr_2O_3(s)+CO=2CrO(l)+CO_2(g)$	182415-43.8T	0.189	1693	1378462	4.54×10^{-4}
			1793	1367117	9.35×10^{-4}
$CrO(l)+CO=Cr(s)+CO_2(g)$	53211+21.4T	0.3778	1693	-543252	1.73×10^{-3}
			1793	-536328	2.13×10^{-3}
$MgCr_2O_4(s)+CO=MgO(s)+2CrO(l)+CO_2(g)$	225260-50.9T	0.0539	1693	1415200	5.07×10^{-5}
			1793	1403765	1.24×10^{-4}
$CrO(l)+CO=Cr(s)+CO_2(g)$	53211+21.4T	0.1078	1693	-543252	1.73×10^{-3}
			1793	-536328	2.13×10^{-3}

actant gas CO is first transferred from the bulk gas stream, it diffuses through the pores between the grains, and further diffuses through a solid product layer within each grain, and then reacts at the spherical reaction interface. The generated product gas CO_2 diffuses backward through the solid product layer, and between the grains and finally transfer into the bulk gas stream. The overall rate of reaction is computed by summing up the contributions of all these individual grains.

If we express the gas reactant CO by A, the solid reactant chromite by B, the solid product by C, and the gas product by D, the reaction can be described as follows:

$$A(g) + bB(s) = cC(s) + dD(g) \tag{1}$$

In this reaction model, it is assumed that the initial pellet size is maintained throughout the reaction. The structure of the porous matrix of the pellet normally will be altered by the chemical reaction and by sintering. The allowance is made up by considering the porosity and thus the tortuosity changes, i.e., the effect on the effective diffusivity. The unreacted core model describes the behaviour of a small particle, and the reaction between the gas and the solid is a reversible reaction of the first order. The schematic diagram of the structure of the grain model is shown in Fig. 2, in which R is pellet radial coordinate, r is the grain reaction front, and C_A is CO concentration.

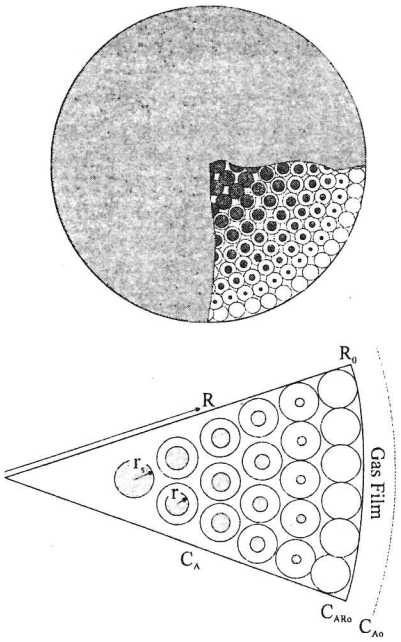

Fig.2. Schematic diagram of the grain model.

At the quasi-steady state, the equimolar counter diffusion is assumed. The amount of gaseous reactant within the pores is negligible compared with the net input and the rate of reaction. ρ_m is molar density of the reducible oxygen in the initial chromite particle. P_0 is the pellet initial total porosity. The governing equations of the model can be obtained as the following two differential equations:

$$\frac{dr}{dt} = -\frac{k}{\rho_m}(C_A \cdot (1 + \frac{D_A^e}{D_D^e \cdot K_E}) - \frac{1}{K_E}(C_{A_o} + (\frac{D_A^e}{D_D^e} - 1) \cdot C_{A_{R_o}})) \tag{2}$$

$$\frac{D_A^e}{R^2}\frac{\partial}{\partial R}(R^2 \frac{\partial C_A}{\partial R}) = 3(1 - P_0)\frac{r^2}{r_s^3}k(C_A \cdot (1 + \frac{D_A^e}{D_D^e \cdot K_E}) - \frac{1}{K_E}(C_{A_o} + (\frac{D_A^e}{D_D^e} - 1) \cdot C_{A_{R_o}})) \tag{3}$$

Here, k, the general reaction rate constant of the chromite grain, can be expressed as follows according to the unreacted core model,

$$\frac{1}{k} = \frac{1}{k_+} + \frac{r(r_s - r)}{r_s}(1 + \frac{D_{AR}^e}{D_{Dg}^e K_E})\frac{1}{D_{AR}^e} \tag{4}$$

k_+ is the forward chemical reaction rate constant, K_E is the general equilibrium constant of chromite reduction with CO, D_{Ag}^e and D_{Dg}^e are the effective diffusivities of CO and CO_2 through the product layer of the chromite grain, respectively.

The relationship between the reaction extent and the reaction time correlated to the experimental measurement can be illustrated as:

$$X = \frac{3}{R_o^3}\int_0^{R_o} R^2(1 - \frac{r^3}{r_s^3})dR \tag{5}$$

Consideration of Heat Transfer

Due to the chemical reaction heat, the temperature of the pellet can be different from that of the gas stream. When the pellet is assumed to be at a uniform temperature at any given time if the reaction heat is relatively small, i.e., the temperature gradient inside the pellet is negligible, the following thermal balance can be formulated:

$$\frac{dT}{dt} = -\frac{\Delta H}{C_p}\frac{dX}{dt} - \frac{3}{R_o(1 - P_0)\rho_m C_p}(h_t(T - T_E) + e\sigma(T^4 - T_E^4)) \tag{6}$$

where, T and T_E are the pellet and environmental temperatures in absolute unit, respectively. At $t=0$, $T=T_E$. ΔH is the chemical reaction heat, C_p is the pellet heat capacity which could be calculated by the heat capacities of solid reactant and product, i.e., $C_p = C_p^B + X(C_p^C - C_p^B)$. h_t is the heat transfer coefficient, e is the emissivity of the pellet surface, and σ is the Stefan-Boltzmann constant.

Initial and Boundary Conditions

It is assumed that no reaction is occurred before $t=0$, there is a symmetrical concentration profile at the centre of the pellet, and the molar flux at the outer surface of the pellet is continuous. Thus, the following initial and boundary conditions can be derived:

At $t=0$, $r(R) = r_s$ (7)

At $R=0$, $\frac{\partial C_A}{\partial R} = 0$ (8)

At $R=R_o$, $D_A^e \frac{\partial C_A}{\partial R} = h_m(C_{A_o} - C_A)$ (9)

Here, h_m is the mass transfer coefficient from the bulk gas stream to the solid sample. C_{A_o} is the gas concentration in the bulk gas stream.

The concentration profile, the movement of the reaction fronts of the chromite grains, the temperature change of the pellet during the reduction and the reduction extent can be calculated by solving the above equations using a finite difference technique.

Model Parameters

Most of the model parameters are evaluated according to the experimental conditions or from the known correlation in the literature, only the chemical reaction rate constant k_+, and its associated activation energy E_A have to be determined experimentally in the present reaction model, listed in Table 2.

Table 2. Model Parameters Used in the Model Calculation

Symbol	Value	Note
R	0.6 cm	measured (7)
r_s	30 μm	
P_g	0.10	grain porosity (7, 11, 12)
P_0	0.30 for green pellet	initial total porosity
P_0	0.28 for sintered pellet	
P_0^o	0.20 for sintered pellet	initial open porosity
P^o	$P_0^o \times (1-2.07\times10^5 exp(-43000/T)\times t)$	open porosity of the pellet
τ_g	35	tortuosity estimated
τ_p	3.5 for green pellet	based on related
τ_p	7 for sintered pellet	porosity values (13)
ρ_m	0.0422 mole/cm^3, green pellet	calculated according to
ρ_m	0.0573 mole/cm^3, sintered pellet	pellet compositions
C_p^B	200.1 J/K·mole	approximated average value
C_p^C	112.6 J/K·mole	based on compositions (9)
C_{A_o}	6.8×10^{-6} mole/cm^3 at 1793K	$C=p/R'T$
C_{A_o}	7.2×10^{-6} mole/cm^3 at 1693K	R'=82.07 cm^3·atm/K·mole
D_{AD}^e	$f(M_A, M_D, T, p, \sigma_{AD}, \Omega_{AD}, P^o, \tau)$	calculated according to
D_{AK}^e	$f(M_A, T, r_s, P^o, \tau)$	Chapman-Enskog Eq. (14)
D_{DK}^e	$f(M_D, T, r_s, P^o, \tau)$	and Dust Gas Model (15)
D_A^e	$1/D_A^e=1/D_{AD}^e+1/D_{AK}^e$	combined eff. of molecular
D_D^e	$1/D_D^e=1/D_{AD}^e+1/D_{DK}^e$	and Knudsen diffusion,
D_{Ag}^e	$1/D_{Ag}^e=1/D_{AD}^e+1/D_{AK}^e$	influenced by porosity and
D_{Dg}^e	$1/D_{Dg}^e=1/D_{AD}^e+1/D_{DK}^e$	tortuosity of solid phase
h_m	8.77 cm/s at 1793K	$Sh=2.0+0.60(Re)^{1/2}(Sc)^{1/3}$
h_m	8.08 cm/s at 1693K	
h_t	2.72×10^{-3} J/s·cm^2·K at 1793K	$Nu=2.0+0.60(Re)^{1/2}(Pr)^{1/3}$
h_t	2.66×10^{-3} J/s·cm^2·K at 1693K	
e	0.8	estimated
K_E	f(X, T)	from K_E^i, ρ_m^i/ρ_m,
ΔH	78020 J at 1793K	$H(T)=H(T_o)+\int C_p(T)dT$
ΔH	77869 J at 1693K	$\Delta H=\sum(\rho/\rho_m)\Delta H_i$
k_+	$9.30\times10^{-3}\cdot exp(-3271.3/T)$, cm/s	experimental data fitting
E_A	27170 J	for green pellet
k_+	$4.16\times10^{6}\cdot exp(-37745/T)$, cm/s	experimental data fitting
E_A	313500 J	for sintered pellet

By considering the sintering effect, the relationship among the porosity, temperature and reduction time was derived based on the experimental analysis on the porosity of the reduced pellets under different experimental conditions (7, 11, 12). The thermophysical properties of CO were extrapolated from the data at lower temperature (16). The equilibrium constants of the chemical reaction of different reducible constitutes in chromite with CO and the reduction steps have been taken into consideration in the establishment of the general equilibrium constant.

Usually, in gas-solid reactions the solid body may swell or shrink. For chromite pellet reduction, according to the experimental observations the chromite grains and the pellet didn't have significant volume changes. During the reduction and sintering, the silicate phase was softened and melted. Thus it is assumed that the open porosity of the pellet was decreased, and so was the effective diffusivities of the reacting gas.

Results and discussion

Modelling under experimental conditions

Reduction of green and sintered pellets of Outokumpu Kemi chromite ore were experimentally investigated by the thermogravimetric analysis with 2 l/min CO flow at temperatures of 1693K and 1793K (7, 11). The calculations were carried out for the reaction systems of which the experimental data are available. The calculated reduction rate is compared to the experimental measurements under the experimental conditions, and the results are shown in Figs. 3-4. A good agreement was achieved, especially for green pellet. In the present reaction model, the reaction mechanism can be demonstrated by the concentration profile and the reduction degree along the pellet radius. As examples, the concentration profile of CO, the reaction front movement of the chromite grains inside the pellet are presented in Figs. 5 and 6. According to these calculated results, the chromite pellet reduction with CO is mixed controlled by the pore diffusion, the chemical reaction and the internal product layer diffusion within the chromite grain, as well as the gas phase mass transfer under the present experimental conditions.

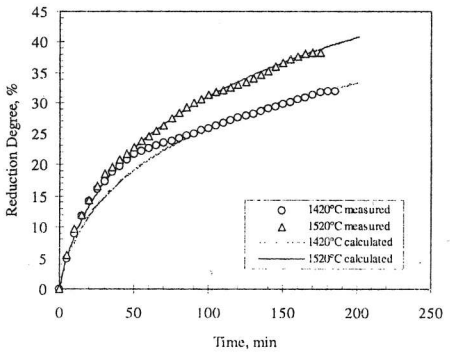

Fig.3. Comparison between measured (7) and calculated reduction rate for green chromite pellet reduction with CO.

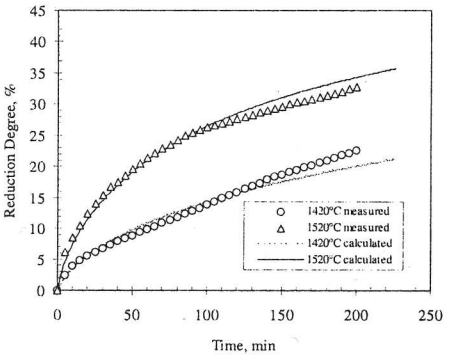

Fig.4. Comparison between measured (11) and calculated reduction rate for sintered chromite pellet reduction with CO.

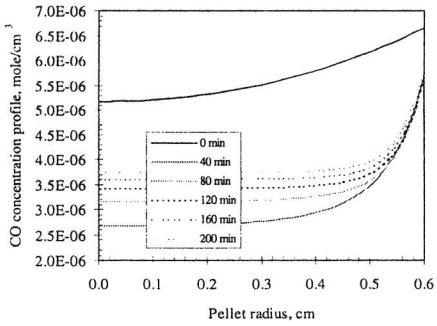

Fig.5. Calculated concentration profile of CO through the pellet for the reduction of green chromite pellet at 1520°C under experimental conditions.

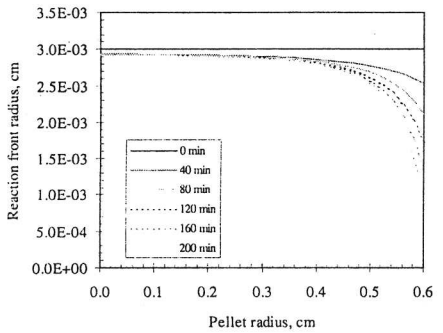

Fig.6. Calculated reaction front radius of chromite grains for the reduction of green chromite pellet at 1520°C under experimental conditions.

The temperature change due to the reaction heat has also been calculated and expressed in Fig.7 for green pellet at 1520°C. Because the general reduction is an endothermic reaction, the temperature of the pellet was decreased quickly in the beginning when the reduction rate is high, and then increased to reach gas stream temperature due to heat transfer.

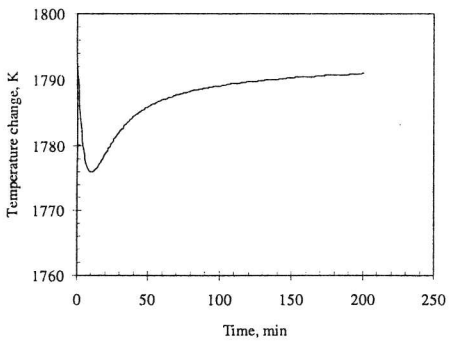

Fig.7. Calculated temperature change during reduction of chromite green pellet with CO at 1520°C under experimental conditions.

According to the model calculation, a diffusional resistance was found to exist within the pellet, a concentration gradient of CO is formed in the pellet, and the reaction rate takes place more rapidly near the pellet surface compared to the pellet interior. This has been verified by the experimental observations which showed that reduction occurred throughout the pellet, but there are gradual composition changes of the Fe/Cr ratio from the analysis of the metal droplets across the pellet. Further, metallic droplets found in the outer part of the pellet were bigger than that in the inner part (7). Certain product layer of the chromite grain was observed experimentally, especially at lower temperature. This provided an evidence for the assumption that the unreacted core model describes the behaviour of the chromite grains within the pellet.

Prediction with different physical parameters of the pellet

The principle parameters to be varied in the real chromite reduction process are the reaction temperature and the structural parameters of the solid agglomerate, such as the porosity, pellet size and the grain size. The latter quantities normally could be changed by modifying the ore preparation and the sintering process. In the present work, the effects of the pellet porosity, pellet size as well as the chromite grain size on the reduction rate were investigated by the model calculations. It is meant to show certain general trends for such reaction systems. The predicted results are illustrated in Figs. 8-10. The porosity has a positive effect on the reduction rate. Increasing the porosity of the chromite pellet will significantly increase the reduction rate. On the other hand, increasing the pellet radius or grain size will decrease the reduction rate.

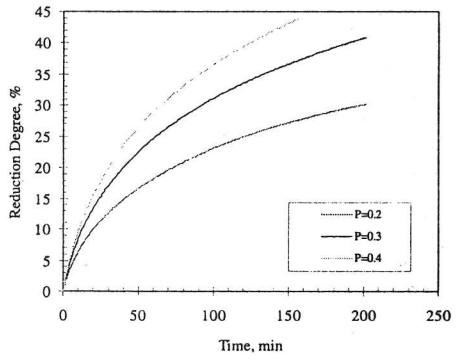

Fig.8. Effect of pellet porosity on reduction rate for the reduction of green chromite pellet at 1520°C.

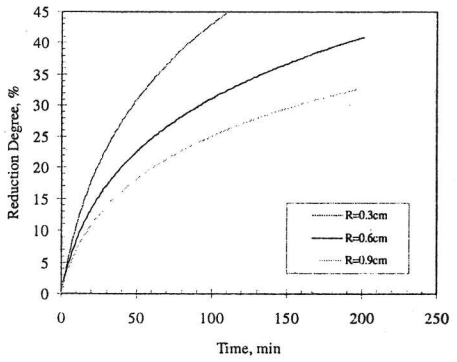

Fig.9. Effect of pellet size on reduction rate for the reduction of green chromite pellet at 1520°C.

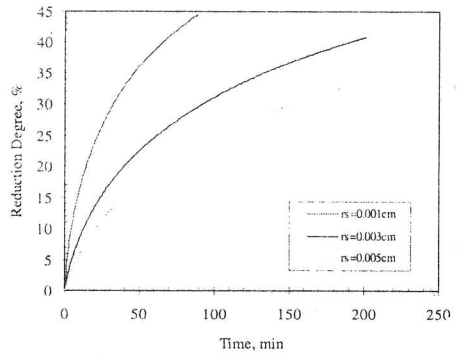

Fig.10. Effect of grain size on reduction rate for the reduction of green chromite pellet at 1520°C.

When changing in larger range, the porosity and the grain size may influence the reaction mechanism. Normally any increase in the porosity is tend to speed up the reaction, except when the chemical reaction is the rate limiting step. Very small grains in principle would result in diffusion control, with the effective pore diffusivity being in the Knudsen region. On the other hand, large grain size would provide a smaller interfacial area for the chemical reaction, causing chemical reaction control even at high values of the rate constant.

Under the present investigation conditions, since the higher reaction rate near the pellet surface, the porosity in the outer part of the pellet decreases more rapidly compared to the inner part of the pellet. This phenomenon has been notified experimentally. The present model didn't take this into account, it is expected to be considered in the next stage modelling work. The chromite grains in the experiment are not actually spherical in shape, and there exists a grain size distribution, it would be possible to improve the model by introducing a shape factor and a grain size distribution, in the future.

Summary

In the present work, the thermodynamic reduction possibility of the reducible constitutes in the chromite was analysed based on chromite composition and the reaction Gibbs free energy. High CO partial pressure is essential for chromite reduction at the temperature range of 1400°C - 1600°C. Iron oxides may be reduced more easily than chromium oxides.

A modified structural grain model was developed which describes the chromite pellet reduction with CO. The overall reaction rate was determined by summing up the contributions from all constituted grains of the pellet. There are a group of differential equations to describe the individual grain reaction, the diffusion of the reactant and product gas within the porous chromite pellet, the mass and heat transfer in the pellet gas film. The model parameters associated with the conditions of the reaction system and the properties of solid and gas reactants were evaluated under interested experimental conditions. Sintering effect was considered by correlating the porosity change of the pellet during the reduction. The general chemical reaction was contributed by all the reducible constitutes in the chromite. The calculated reduction rate was compared to the experimental measurement, and acceptable agreement was obtained. According to the discussion on the reaction mechanism of the reduction of chromite pellet with CO, it is concluded that chromite pellet reduction with CO is mixed controlled by chemical reaction, internal diffusion through the product layer of chromite grain, pore diffusion within the pellet and even the gas phase mass transfer under the experimental conditions. In addition, the effects of the pellet characteristics were predicted based on the model calculations.

Acknowledgements

The authors are grateful to the SULA 2 energy research program (TEKES) for financial support.

References

1. O. Levenspiel, Chemical Reaction Engineering. 2nd ed. (New York, NY: John Wiley and Sons Inc., 1962).
2. M. Ishida and C.Y. Wen, "Comparison of Kinetic and Diffusional Models for Solid-Gas Reactions", AIChE J., 14(2)(1968), 311-317.
3. J.H. Bowen and C.K. Cheng, "A Diffuse Interface Model for Fluid-Solid Reactions", Chem. Eng. Sci., 24(1969), 1829 - 1831.
4. S.K. Bhatia and D.D. Perlmutter, "A Random Pore Model for Fluid-Solid Reactions", AIChE J., 27(2)(1981), 247-254.
5. B. Linder and D. Simonsson, "Comparison of Structural Models for gas-Solid Reactions in Porous Solids Undergoing Structural Changes", Chem. Eng. Sci., 36(1981), 1519-1527.
6. P.A. Ramachandran and M.P. Dudukovic, "Reactions of Solid Particles with Nonuniform Distribution of Solid Reactant", Chem. Eng. Sci., 39(1984), 669-680.
7. M. Kekkonen, Y. Xiao and L. Holappa, "Kinetic Study on Solid State Reduction of Chromite Pellets" (INFACON 7 Conference Proceedings, Trondheim, Norway, June 11-14, 1995), 351-360.
8. E.T. Turkdogan, Physical Chemistry of High Temperature Technology (London: Academic press, 1980)
9. O. Knacke, O. Kubaschewski and K. Hesselmann, Thermochemical Properties of Inorganic Substances. 2nd ed. (Springer-Verlag Berlin, Heidelberg, New York, 1991).
10. S.S. McRae, "An Investigation into Pelletizing and Prereduction of Transvaal Chromites" (Proceedings of the 2nd International Symposium on Agglomeration, Atlanta, March 6-10, Vol.1, 1977), 356-377.
11. M. Kekkonen, L. Holappa and P. Niemela (To be presented in INFACON 8 Conference, Beijing, China, June 7-10, 1998).
12. A. Syynimaa, "The Effect of Oxidation State on the Reduction of Sintered Chromite Pellets" (M.Sc Thesis, Helsinki University of Technology, 1996).
13. K.K. Kim and J.M. Smith, "Diffusion in Nickel Oxide Pellets - Effects of Sintering and Reduction", AIChE J., 20(4)(1974), 670 - 678.
14. J.O. Hirschfelder, C.F. Curtiss and R.B. Bird, Molecular Theory of Gases and Liquids (New York: Wiley, 1956).
15. E.A. Mason, A.P. Malinauskas and R.B. Evans, "Flow and Molecules", J. of Chemical Physics, 46(8)(1967), 3199-3216.
16. F.P. Incropera and D.P. Dewitt, Fundamentals of Heat and Mass Transfer, 3rd ed. (Singapore: John Wiley & Sons, 1990).